

# Pascal (Yang Hui) triangles and power laws in the logistic map

Carlos Velarde<sup>1</sup>, Alberto Robledo<sup>2</sup>

1. Instituto de Investigaciones en Matemáticas Aplicadas y en Sistemas, Universidad Nacional Autónoma de México

2. Instituto de Física y Centro de Ciencias de la Complejidad, Universidad Nacional Autónoma de México,

Apartado Postal 20-364, México 01000 DF, Mexico.

## Abstract

We point out the joint occurrence of Pascal triangle patterns and power-law scaling in the standard logistic map, or more generally, in unimodal maps. It is known that these features are present in its two types of bifurcation cascades: period and chaotic-band doubling of attractors. Approximate Pascal triangles are exhibited by the sets of lengths of supercycle diameters and by the sets of widths of opening bands. Additionally, power-law scaling manifests along periodic attractor supercycle positions and chaotic band splitting points. Consequently, the attractor at the mutual accumulation point of the doubling cascades, the onset of chaos, displays both Gaussian and power-law distributions. Their combined existence implies both ordinary and exceptional statistical-mechanical descriptions of dynamical properties.

## 1 Introduction

The logistic map has played a prominent role in the development of the field of nonlinear dynamics [1]-[3]. The simplicity of its quadratic expression and the richness and intricacy of the properties that stem from it have captivated a large number of scholars and students over decades. It has served as a standard source for the illustration of nonlinear concepts such as: bifurcations, stable and unstable periodic orbits, periodic windows, ergodic and mixing behaviors, chaotic orbits and universality in the sense of the Renormalization Group (RG) method [1]-[3]. It has also become a suitable model system for the exploration of statistical-mechanical structures [4]. All of these properties are shared by one-dimensional unimodal maps where the quadratic maximum is replaced by an extremum of general nonlinearity  $z > 1$  [2, 5]. Here we concisely draw attention to the presence of geometrical and scaling laws in the family of attractors generated by the logistic map and to the consequences that these laws have in the dynamical properties of their most interesting object of study: the period-doubling transition to chaos. One-dimensional nonlinear maps, like the logistic, are necessarily dissipative [1] and they settle after much iteration into attractors that may consist of a finite set of points regularly visited or an infinite number of points that may be irregularly (or chaotically) visited

[1]-[3]. The logistic map possesses an infinite family of attractors that are connected via cascades of bifurcations at which periods or number of chaotic bands duplicate [1]-[3]. These families of attractors display power laws associated with attractor positions and Pascal Triangles associated with distances between these positions.

We recall that a Pascal Triangle is a triangular arrangement of the binomial coefficients and that it contains many remarkable numerical relations [6]. Blaise Pascal studied this array in the 17th century, although it had been described centuries earlier by the Chinese mathematician Yang Hui, and then by other Indian and Persian scholars. It is therefore known as the Yang Hui triangle in China [7]. This triangle serves as the basis of the De Moivre-Laplace theorem [8] an earlier limited version of the central limit theorem leading to the Gaussian distribution.

We provide below a description of how these properties arise in the logistic map and discuss their implications for the mathematical structures in the dynamics of this nonlinear system, itself a convenient numerical laboratory for the study of statistical-mechanical theories [4].

## 2 The bifurcation cascades of the logistic map

We briefly recall the basic definitions of the superstable periodic attractors (or supercycles) and the chaotic band-merging attractors (or Misiurewicz points) [1]-[3]. These have become convenient families of attractors in formal descriptions of the bifurcation cascades of unimodal maps, often illustrated by the logistic map  $f_\mu(x) = 1 - \mu x^2$ ,  $-1 \leq x \leq 1$ ,  $0 \leq \mu \leq 2$ .

The superstable orbits of periods  $2^n$ ,  $n = 1, 2, 3, \dots$ , are located along the bifurcation forks, i.e. the control parameter value  $\mu = \bar{\mu}_n < \mu_\infty$  for the superstable  $2^n$ -attractor is that for which the orbit of period  $2^n$  contains the point  $x = 0$ , where  $\mu_\infty = 1.401155189\dots$  is the value of  $\mu$  at the main period-doubling accumulation point. The positions (or phases) of the  $2^n$ -attractor are given by  $x_m = f_{\bar{\mu}_n}^{(m)}(0)$ ,  $m = 0, 1, \dots, 2^n - 1$ . The diameters  $d_{n,m}$  are defined as  $d_{n,m} \equiv x_m - f_{\bar{\mu}_n}^{(2^n-1)}(x_m)$  [1]. See Fig. 1. Notice that infinitely many other sequences of superstable attractors appear at the period-doubling cascades within the windows of periodic attractors for values of  $\mu > \mu_\infty$  [1].

When  $\mu$  is shifted to values larger than  $\mu_\infty$ ,  $\Delta\mu \equiv \mu - \mu_\infty > 0$ , the attractors are chaotic and consist of  $2^n$  bands,  $n = 0, 1, 2, \dots$ , where  $2^n \sim \Delta\mu^{-\kappa}$ ,  $\kappa = \ln 2 / \ln \delta$ , and  $\delta = 4.669201609102\dots$  is the universal constant that measures both the rate of convergence of the values of  $\mu = \bar{\mu}_n$  to  $\mu_\infty$  at period doubling or at band splitting points or Misiurewicz points [2]. The Misiurewicz ( $M_n$ ) points are attractor merging crises, where multiple pieces of an attractor merge together at the position of an unstable periodic orbit. The  $M_n$  points can be determined by evaluation of the trajectories with initial condition  $x_0 = 0$  for different values of  $\mu$ , as these orbits follow the edges of the chaotic bands until at  $\mu = \hat{\mu}_n$ , the control parameter value for the  $M_n$  point, the unstable orbit of period  $2^n$  reaches the merging crises [9]. See Fig. 2. Notice that infinitely many other sequences of Misiurewicz points appear at the band-splitting cascades within the windows of periodic attractors for values of  $\mu > \mu_\infty$  [1].

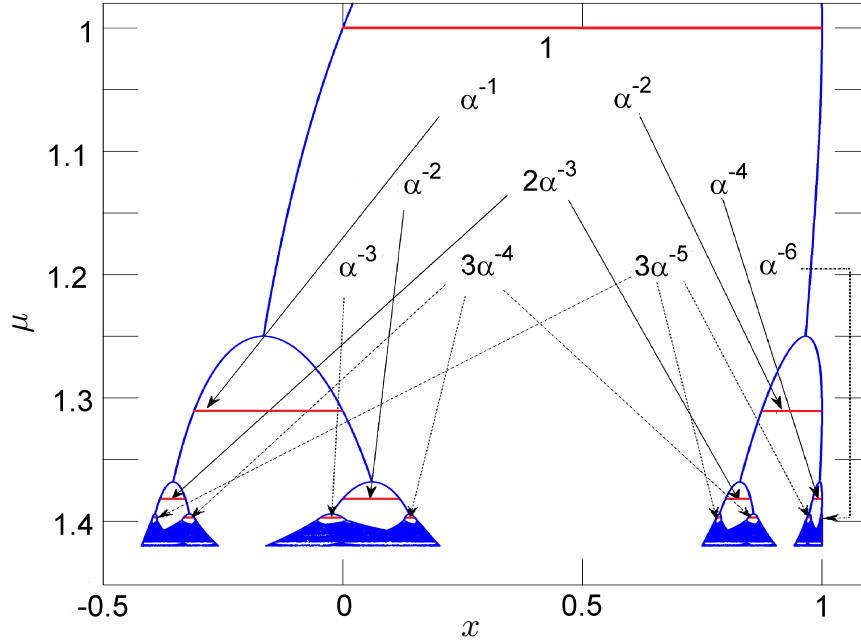


Figure 1: Sector of the period-doubling bifurcation tree for the logistic map  $f_\mu(x)$  that shows the formation of a Pascal Triangle of diameter lengths according to the binomial approximation explained in the text, where  $\alpha \simeq 2.50291$  is the absolute value of Feigenbaum's universal constant.

### 3 Pascal Triangles and power-law scaling

The Pascal Triangles and the power-law scaling present in the families of attractors along the bifurcation cascades of the logistic map are best appreciated graphically. These can be visualized in Figs. 1 to 4 that we describe below.

Fig. 1 shows the main period-doubling cascade for the logistic map  $f_\mu(x)$  in the  $(x, \mu)$  plane from period two to its accumulation point (the transition to chaos) and beyond. A few of the supercycle diameters are shown and their approximate sizes are annotated as inverse powers of the (absolute value of the) universal constant  $\alpha = -2.50291 \dots$ . For convenience we denote  $|\alpha|$  as  $\alpha$  below and in the figure captions. The diameters naturally assemble into well-defined size groups and the numbers of them in each group can be precisely arranged into a Pascal Triangle. In fact, the diameter lengths within each group are not equal, however the differences in lengths within groups diminishes rapidly as the period  $2^n$  increases [10]. A detailed study of the quantitative differences between the values of the diameters generated by the logistic map and those obtained from the binomial approximation that form the Pascal triangle in Fig. 1 is given in [10]. There are two groups with only one member, the largest and the shortest diameters, and the numbers within each group are given by the binomial coefficients.

Fig. 2 shows a segment of the main band-splitting cascade of the logistic map  $f_\mu(x)$  in the  $(x, \mu)$  plane where we indicate the widths of these bands at the control parameter values  $\hat{\mu}_n$  when they each split into two new bands. As in the case of the diameters the band widths diminish in size according to the same inverse powers of  $\alpha$  as their numbers  $2^n$  increase. They also form groups of nearly equal sizes with numbers given by the binomial coefficients. Again if it is assumed that for every value of  $n$  the widths of comparable

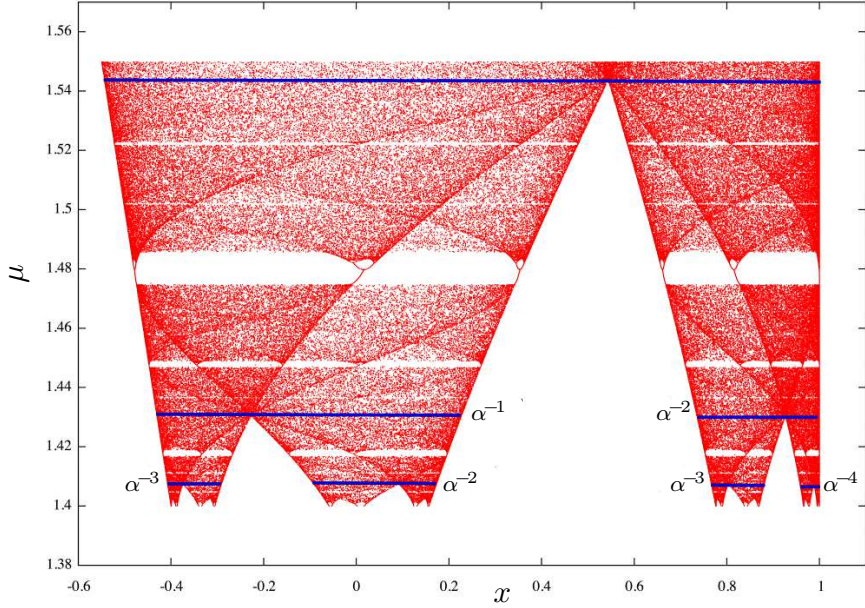


Figure 2: Sector of the main band-splitting cascade for the logistic map  $f_\mu(x)$  that shows the formation of a Pascal triangle of band widths (solid lines) at splitting according to the scaling approximation explained in the text, where  $\alpha \simeq 2.50291$  is the absolute value of Feigenbaum's universal constant.

lengths have equal lengths then these widths can be obtained from the widths of shortest and longest lengths via a simple scale factor consisting of an inverse power of  $\alpha$ . Under this approximation we observe a Pascal Triangle across the band-splitting cascade.

Fig. 3 shows the period-doubling cascade for the logistic map  $f_\mu(x)$  in logarithmic scales in order that the power-law scaling of positions of trajectories along the supercycle attractors is plainly observed. These positions are shown as circles. As it can be appreciated in the figure certain sequences of positions each belonging different cycles fall on straight lines that share a common slope. One such alignment corresponds to positions of the principal diameters  $d_{n,0}$  that are formed when  $x = 0$  is the other endpoint of the interval. (The positions at  $x = 0$  do not appear in the figure as their logarithm is minus infinity). The power-law scaling is of the form  $|x| \sim \alpha^{-n}$ .

Fig. 4 shows the band-doubling cascade of chaotic attractors in the logistic map  $f_\mu(x)$  in logarithmic scales so that the power-law scaling of splitting positions  $M_n$  is clearly observed. Some of these positions are shown as circles. As it can be observed in the figure sequences of Misiurewicz points fall on straight lines that share a common slope. The power-law scaling is again of the form  $|x| \sim \alpha^{-n}$ .

## 4 Gaussian and multi-scale distributions

As mentioned, the Pascal Triangle is closely associated with a special case of the Central Limit Theorem, known as the De Moivre-Laplace theorem that dates back to 1870 [8]. This theorem establishes that the limiting form of the binomial distribution, the sum of the binomial series of  $(p + q)^n$  for which the number of successes  $s$  falls between  $p$  and  $q$ ,  $p + q = 1$ , is the Gaussian distribution. Therefore the occurrences of approximate Pascal

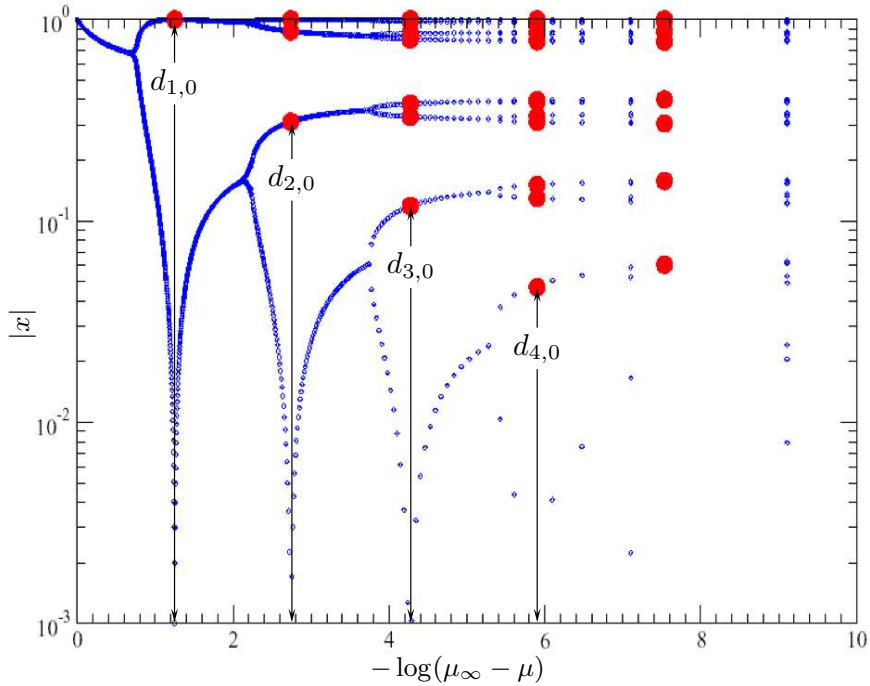


Figure 3: Absolute value of attractor positions for the logistic map  $f_\mu(x)$  in logarithmic scale as a function of the logarithm of the control parameter difference  $\mu_\infty - \mu$ . The supercycle attractors are shown by the arrows and the notation  $d_{1,0}, d_{2,0}, \dots$  corresponds to the so-called principal diameters, the distances between  $x = 0$ , the position of the maximum of the map, and the nearest cycle position.

Triangles for the sets of diameters and bandwidths in the bifurcation cascades implies a Gaussian distribution for these lengths at their accumulation point, the period-doubling onset of chaos. On the other hand, the power-law scaling of supercycle and band-splitting positions is reflected onto the period-doubling onset of chaos as a complete organization of subsequences of positions each following the same power-law scaling. Iteration time evolution at  $\mu_\infty$  from  $t = 0$  up to  $t \rightarrow \infty$  traces the period-doubling cascade progression from  $\mu = 0$  up to  $\mu_\infty$ . There is a quantitative relationship between the two developments. Specifically, the trajectory inside the attractor at  $\mu_\infty$  with initial condition  $x_0 = 0$ , the  $2^\infty$ -supercycle orbit, takes positions  $x_t$ , such that the distances between appropriate pairs of them reproduce the diameters  $d_{n,m}$ , defined for the supercycle orbits with  $\bar{\mu}_n < \mu_\infty$  [4]. See Fig. 5, where the absolute value of positions and logarithmic scales are used to illustrate the equivalence.

The limit distributions of sums of positions at the period-doubling transition to chaos in unimodal maps have been studied by making use of the trajectory properties described above [11], [12]. Firstly, the sum of positions as they are visited by a single trajectory within the attractor was found to have a multifractal structure imprinted by that of the accumulation point attractor [11]. It was shown, analytically and numerically, that the sum of values of positions display discrete scale invariance fixed jointly by the universal constant  $\alpha$ , and by the period doublings contained in the number of summands. The stationary distribution associated with this sum has a multifractal support given by the period-doubling accumulation point attractor [11]. Secondly, the sum of subsequent po-

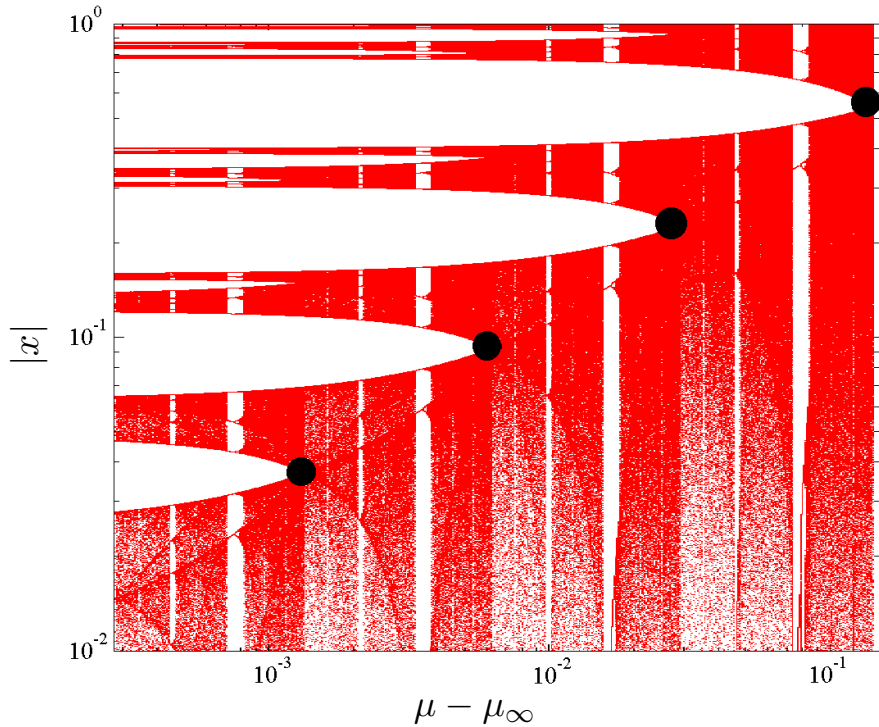


Figure 4: Attractor bands and gaps between them (white horizontal regions) in logarithmic scales,  $-\log(\mu - \mu_\infty)$  and  $\log(|x|)$  in the horizontal and vertical axes, respectively. The band-splitting points  $M_n$  (circles) follow a straight line indicative of power-law scaling. The vertical white strips are periodic attractor windows.

sitions generated by an ensemble of uniformly distributed initial conditions in the entire phase space was recently determined [12]. It was found that this sum acquires features of the repeller preimage structure that dominates the dynamics toward the attractor. The stationary distribution associated with this ensemble has a hierarchical structure with multi-scale properties [12]. See also Ref. [13].

## 5 Scale invariant properties and statistical-mechanical structures

Underlying the power-law scaling of positions are the self-affine properties that permeate the dynamics of unimodal maps. As we have seen, these properties manifest visibly along the well-known bifurcation cascades described here. They are also at the center of the Renormalization Group (RG) functional composition developed time ago [1] to provide a firm theoretical basis to the universal properties of the accumulation point of the bifurcation cascades. The RG fixed-point map  $f^*(x)$  satisfies the condition  $f^*(f^*(x)) = \alpha f^*(x/\alpha)$ . Fig. 5 offers us a simple visual opportunity to observe the effect of the RG functional composition and its fixed-point map property. First we notice that certain position subsequences appear aligned in the figure. The most visible is that of  $|x_t|$ ,  $t = 2^n$ ,  $n = 0, 1, 2, 3, \dots$ , with a slope equal to  $\ln \alpha / \ln 2$ , the main diagonal pattern in the figure. Next to it is the subsequence  $|x_t|$ ,  $t = 3 \times 2^n$ ,  $n = 0, 1, 2, 3, \dots$ , with the same slope,

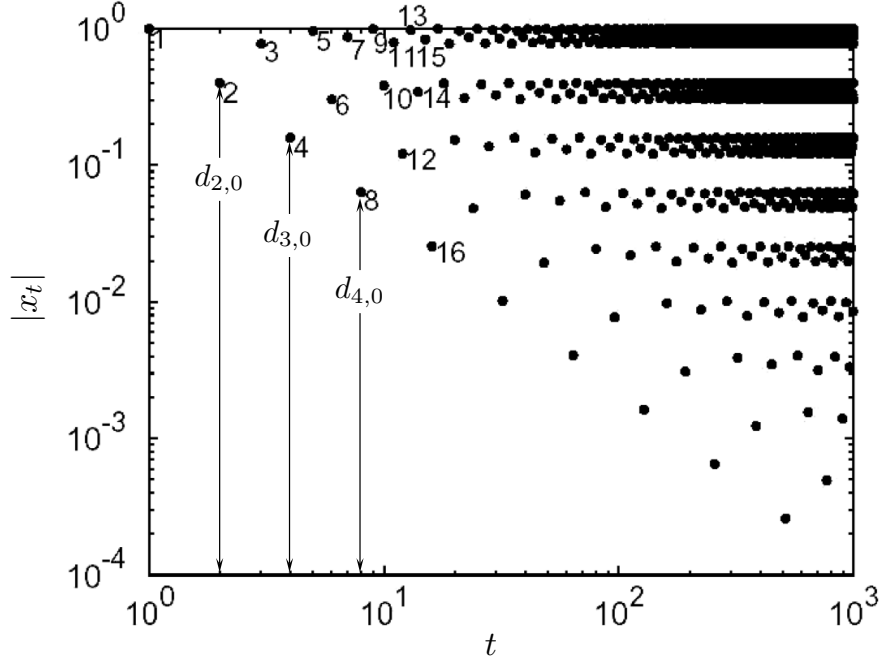


Figure 5: Absolute value of trajectory positions  $x_t$ ,  $t = 0, 1, \dots$ , for the logistic map  $f_\mu(x)$  at  $\mu_\infty$ , with initial condition  $x_0 = 0$ , in logarithmic scale as a function of the logarithm of the time  $t$ , also shown by the numbers close to the points.

and so on. All the positions  $x_t$  can be distributed into subsequences of the form  $|x_t|$ ,  $t = (2l + 1)2^n$ ,  $n = 0, 1, 2, 3, \dots$ ,  $l = 0, 1, 2, 3, \dots$ , that form a family of lines in the figure with the fixed slope  $-\ln \alpha / \ln 2$  [4]. And all of the infinite family of aligned subsequences of positions can be collapsed onto a single line via rescaling with the use of a “waiting” time  $t_w = 2l + 1$ ,  $l = 0, 1, 2, 3, \dots$ , a property known as aging in the topic of glassy dynamics [4], [14].

We observe that the positions in the logarithmic scales of Fig. 5 appear grouped into horizontal bands separated by gaps of equal widths. The top band contains one half of the attractor positions as all the odd iteration times appear there. The second band is made of one quarter of the attractor positions, those that correspond to iteration times of the form  $t = 2 + 2^n$ ,  $n = 0, 1, 2, 3, \dots$ . And similarly, the  $(k + 1)$ -th band contains  $1/2^k$  of the positions of the attractor, those for iteration times of the form  $t = 2^k + 2^n$ ,  $n = 0, 1, 2, 3, \dots$ ,  $k = 0, 1, 2, 3, \dots$ . The RG method successively transforms the system under study by elimination of degrees of freedom followed by rescaling aimed at restoring its original condition. This procedure can be envisaged in Fig. 5 by eliminating its top band, one half of the total attractor positions, and restoring the original figure by shifting the remaining positions horizontally by an amount  $-\ln 2$  and vertically by an amount  $\ln \alpha$ , in line with the slope  $-\ln \alpha / \ln 2$  of the aligned subsequences. This graphical procedure is equivalent to functional composition. Repeated application of this transformation leads asymptotically to the scaling property of the fixed-point map  $f^*(x)$ .

The scale invariant features of the accumulation point of the bifurcation cascades can be related to statistical-mechanical properties that involve generalized entropy expressions [4], [10].

## Acknowledgements

AR is grateful for the hospitality received from the organizers of SPMCS14 in Yichang, China, and acknowledges support from DGAPA-UNAM-IN103814 and CONACyT-CB-2011-167978 (Mexican Agencies). CV acknowledges the support provided by IIMAS-UNAM.

## References

- [1] Schuster R.C. *Deterministic Chaos. An Introduction*. VCH Publishers, Weinheim. (1988).
- [2] Beck C. and Schlogl F. *Thermodynamics of Chaotic Systems*. Cambridge University Press, Cambridge. (1993).
- [3] Schroeder M. *Fractals, Chaos, Power Laws: Minutes from an Infinite Paradise*. Freeman, New York. (1991).
- [4] Robledo A. *Entropy* **15** 5178, (2013).
- [5] van der Weele J.P., Capel H.W. and Kluiving R. *Physica* **145A** 425, (1987).
- [6] See for example: [http://en.wikipedia.org/wiki/Pascal's\\_triangle](http://en.wikipedia.org/wiki/Pascal's_triangle)
- [7] See for example: [http://en.wikipedia.org/wiki/Yang\\_Hui](http://en.wikipedia.org/wiki/Yang_Hui)
- [8] See for example: [http://en.wikipedia.org/wiki/DeMoivre-Laplace\\_theorem](http://en.wikipedia.org/wiki/DeMoivre-Laplace_theorem)
- [9] Grebogi C., Ott E. and Yorke J. A. *Physica D* **7** 181, (1983).
- [10] Diaz-Ruelas A. and Robledo A. *Europhys. Lett.* **105** 40004, (2014).
- [11] Fuentes M.A. and Robledo A. *J. Stat. Mech.* **P01001**, (2010).
- [12] Fuentes M.A. and Robledo A. *Eur. Phys. J. B* **87** 32, (2014).
- [13] Diaz-Ruelas A., Fuentes M.A. and Robledo A. *Europhys. Lett.* **108** 20008, (2014).
- [14] Robledo A. *Phys. Lett. A* **328** 467, (2004).